energies

MDPI

Review

A Review of Current Advances in Ammonia Combustion from the Fundamentals to Applications in Internal Combustion Engines

Fei Ma [1], Lingyan Guo [1], Zhijie Li [1], Xiaoxiao Zeng [1], Zhencao Zheng [2], Wei Li [1,*], Feiyang Zhao [2,*] and Wenbin Yu [2]

[1] State Key Laboratory of Engine and Powertrain System, Weichai Power Co., Ltd., Weifang 261061, China
[2] School of Energy and Power Engineering, Shandong University, Jinan 250100, China
* Correspondence: liwei09@weichai.com (W.L.); fyzhao@sdu.edu.cn (F.Z.)

Abstract: The energy transition from hydrocarbon-based energy sources to renewable and carbon-free energy sources such as wind, solar and hydrogen is facing increasing demands. The decarbonization of global transportation could come true via applying carbon-free fuel such as ammonia, especially for internal combustion engines (ICEs). Although ammonia has advantages of high hydrogen content, high octane number and safety in storage, it is uninflammable with low laminar burning velocity, thus limiting its direct usage in ICEs. The purpose of this review paper is to provide previous studies and current research on the current technical advances emerging in assisted combustion of ammonia. The limitation of ammonia utilization in ICEs, such as large minimum ignition energy, lower flame speed and more NO_x emission with unburned NH_3, could be solved by oxygen-enriched combustion, ammonia–hydrogen mixed combustion and plasma-assisted combustion (PAC). In dual-fuel or oxygen-enriched NH_3 combustion, accelerated flame propagation speeds are driven by abundant radicals such as H and OH; however, NOx emission should be paid special attention. Furthermore, dissociating NH_3 in situ hydrogen by non-noble metal catalysts or plasma has the potential to replace dual-fuel systems. PAC is able to change classical ignition and extinction S-curves to monotonic stretching, which makes low-temperature ignition possible while leading moderate NO_x emissions. In this review, the underlying fundamental mechanism under these technologies are introduced in detail, providing new insight into overcoming the bottleneck of applying ammonia in ICEs. Finally, the feasibility of ammonia processing as an ICE power source for transport and usage highlights it as an appealing choice for the link between carbon-free energy and power demand.

Keywords: ammonia; internal combustion engines; combustion; emissions

Citation: Ma, F.; Guo, L.; Li, Z.; Zeng, X.; Zheng, Z.; Li, W.; Zhao, F.; Yu, W. A Review of Current Advances in Ammonia Combustion from the Fundamentals to Applications in Internal Combustion Engines. *Energies* **2023**, *16*, 6304. https://doi.org/10.3390/en16176304

Academic Editor: Sergey M. Frolov

Received: 26 July 2023
Revised: 27 August 2023
Accepted: 28 August 2023
Published: 30 August 2023

1. Introduction

Global transition from traditional fossil to renewable resources has been a concern for years to mitigate greenhouse gases. To a large extent, renewable fuels are regarded as promising energy carries particularly adapted for long-distance and high-powered mobility or long-term energy storage. Hydrogen, a carbonless fuel, has been recognized as the most promising fuel and clean energy carrier for automotive, marine and power generation [1]. A global hydrogen-based economy will be a sunrise for the energy issue after solving the bottleneck regarding the transportation and storage of hydrogen with reliable safety and reasonable cost. Therefore, closer attention has been paid to studying H_2-carrier fuel in the form of different chemical substances.

Ammonia (NH_3) is presently receiving a surge of attention as an energy carrier of high gravimetric hydrogen density (17.8% hydrogen content by mass), and is considered a carbon-free fuel that can be directly used in both combustion and fuel cell systems. Ammonia is a colorless gas with a very pungent odor at room temperature and can be dissolved in water. Ammonia has trigonal pyramidal molecule geometry with three hydrogen atoms, as well as an unshared pair of electrons attached to a nitrogen atom, and

molecule polar covalent bond formation takes place between nitrogen and hydrogen [2]. Due to the strong hydrogen bonds between ammonia molecules, it is easily liquefied. Liquefaction of ammonia is able to happen at 10 bar at room temperature or −33.4 °C at atmospheric pressure, while hydrogen can only be liquefied under −253 °C. Ammonia is able to be stored in liquid form under suitable pressure conditions, ensuring a comparable energy density with other fuels, and it has competitive lower heating value (LHV) [3]. In terms of energy density in storage conditions, liquid ammonia is more than 40% denser than liquid hydrogen or more than twice that of compressed gas hydrogen.

Ammonia is the second-largest chemical products (after sulfuric acid) in the world (over 200 million tons per annum globally with more than USD $60 billion market value) [4,5]. Approximately 80% of global ammonia is utilized in agriculture as fertilizer, with around 5% for explosives, and the balance for industrial cooler refrigerant and chemical commodities. Currently, little ammonia is utilized for energy carriage, but there is definitely great potential for ammonia to be consumed as a renewable fuel in gas turbines, internal combustion engines or fuel cells without a carbon footprint in the years to come. The industrial production of ammonia (NH_3) from N_2 and H_2 is mainly dominated by the Haber–Bosch (H-B) process in the presence of metal catalyst at high temperature (~700 K) and 10–25 MPa, responsible for 1.2% of the global anthropogenic CO_2 emissions [6]. The energy consumption of green H-B is within the range of 27.4–31.8 GJ $t_{NH3}{}^{-1}$, and improvement in overall energy efficiency up to 65% [7]. Furthermore, ammonia could be manufactured from renewable energy sources such as biomass, wind or solar. Achieving a CO_2-free, energy-efficient, low-capital Haber–Bosch synthesis loop is under investigation by electrically driven [8] or electrochemical [9] power sources. In addition, because the absorption and desorption reactions of ammonia is fully reversible, ammonia is able to be released from a solid complex such as $Mg(NH_3)_6Cl_2$ upon heating and compacted into a dense shape, which makes storage simple and safe [10]. Some of the metal ammine complexes show promising results for storing hydrogen, for example, $Mg(NH_3)_6Cl_2$ can store over 9% hydrogen by weight in its solid form. Therefore, ammonia is considered a superb fuel due to its carbon-free structure, safe storage and transportation and low production cost, but with high hydrogen gravimetric density.

Ammonia has regained a great deal of interest from governments and institutes, since it not only enables the vital delivery of nitrogen needed for crop growth but also serves as a chemical that is capable of producing cooling, heating, power, and propulsion with minimum storage cost [11]. When ammonia is labeled as one of the carbon-free alternative fuels, the interest in deploying ammonia is in fast growth. Herbinet et al. [12] summarized an interesting comparison between the advantages and disadvantages of ammonia when used as power solutions. Gas turbines are the system of choice for large-scale ammonia utilization, while solid oxide fuel cells perform better at small scales (below 10 MW). Ammonia can also be directly used in both spark ignition engines or compression ignition engines [12,13]. Predicted by life cycle analysis, it will reduce greenhouse gas emissions by three times through ammonia-fueled vehicles as an alternative to conventional gasoline [14]. The UK Department for Transport proposed taking action on clean maritime growth by placing "a group of hydrogen or ammonia powered domestic vessels in operation" [15]. Indeed, ammonia has a higher octane number than gasoline and natural gas (Table 1), thus allowing a higher compression ratio applied in engine operation. Even though the energy density of compressed ammonia is comparably less than that of gasoline and diesel, it is still much higher than that of compressed natural gas or liquid hydrogen. Research on ammonia for internal combustion engines (ICEs) is in its early stages. Ammonia has extreme low combustion intensity with difficult flammability, reflected by its narrow flammability limits and low laminar burning velocity (Table 1).

Table 1. The main characteristics of some fuels [16,17].

Properties	Units	Ammonia	Hydrogen	Hydrogen	Natural Gas	Gasoline	Diesel	Methanol	Ethanol
Molecular formula		NH_3	H_2	H_2	CH_4	C_5H_{12}-$C_{12}H_{26}$	C_4H_{100}-$C_{12}H_{26}$	CH_3OH	C_2H_5OH
Density	@NTP (kg/cm^3)	0.73		0.083	0.66	700–780	830–855	791	785
Boiling point	(°C)	−33		−253	−161.5	33–190	180–370	64.7	78
Evaporation latent heat	(kJ/kg)	1370		446	511	305	230–250	1160	840
Low heating value	(MJ/kg)	18.8	120.0	120.0	50.0	44.0	42.6	19.6	26.8
Laminar flame velocity	@NTP (cm/s)	7		100–1000	36.53	50	86.5	50	47
Carbon atomic mass fraction	(wt%)	0	0	0	75	86.5	86.3	37.5	52.1
Hydrogen atomic mass fraction	(wt%)	17.6	100	100	25	13.5	13.1	12.5	13
Storage method		Compressed Liquid	Compressed Liquid	Compressed Gas	Compressed Liquid	Liquid	Liquid		
Storage temperature	(K)	298	20	298	298	298	298		
Energy density under storage	(MJ/L)	11.5	8	4.8	9.7	32.0	35.2		21.3
Autoignition temperature	(K)	924	844/824	844/824	723/885	573	503/499–506	737	696
Minimum ignition energy	(mJ)	8		0.02	0.28	0.2–0.3		0.14	0.28
Octane rating	(RON)	110/≥130	>130/≥130	>130/≥130	107/125	90–98/92–98		109	109

NTP: Normal temperature and pressure condition: P = 1 bar, T = 293.15 K.

2. Method of Ammonia Production

Ammonia production can be classified as brown (or gray) ammonia, blue ammonia and green ammonia based on the carbon emissions from the manufacturing process [18]. Current brown ammonia is massively produced by reforming hydrocarbons such as methane using proven Haber–Bosch industrial technology [19], which requires a high-temperature, high-pressure environment as well as addition of N_2, as shown in Figure 1. Blue ammonia is able to be generated using hydrogen from natural gas in conjunction with CCUS (carbon capture, utilization, and storage), while the most desirable green ammonia can be made using hydrogen from water electrolysis without CO_2 emissions. Overall, the majority of ammonia (around 86% to 96%) is manufactured through the traditional Haber–Bosch process, although it is energy-intensive with low conversion efficiency (25% at 30 MPa) and high carbon emissions [20]. In addition, the remaining commercial ammonia comes from alternative technologies such as electrochemical or thermochemical processes etc. [19,20] powered by low pressure and no catalysts with carbon-free emissions [21]. Moreover, the electrochemical process can be performed over a wide range of temperatures, depending on the electrolyte applied during the process [19].

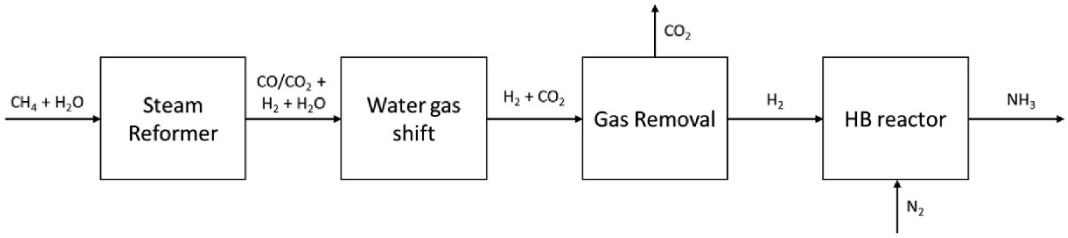

Figure 1. Simplified NH_3 production progress with CH_4 as the main raw material [19].

Plasma-assisted ammonia synthesis is alternative option to produce NH_3 from H_2 and N_2 via the formation of NH radicals. Many studies have concentrated on the application of plasma catalysts at ambient temperature. Li et al. [22] found that the reaction rate of ammonia synthesis was facilitated by the interaction between catalyst and plasma, which was double the pure catalyst load and 30 times that of plasma only. Andersen et al. [23] and Sun et al. [24] used the open-source code ZDPlasKin to numerically figure out the underlying kinetic processes of plasma-assisted ammonia synthesis. They both found surface interactions such as Eley–Rideal (E-R) and Langmuir–Hinshelwood (L-H) reactions contributed to the production of ammonia significantly. The dominant reaction mechanisms of plasma-catalyzed ammonia synthesis are illustrated in Figure 2 and were summarized by Engelmann et al. [25]. Due to electron collisions, a large number of N_2 and H_2 molecules were ionized, excited, adsorbed and dissociated, followed by the adsorption of free radicals (N, H, NH and NH_2) on the surface of the catalyst. After that, these particles in the adsorbed state either underwent E-R reactions with groups in the gas phase or LH reactions on the catalyst surface due to atomic diffusion. Eventually, the resulting NH_3 was released from the catalyst surface. Unlike the traditional H-B process, breakage of the NN triple bond can happen at room temperature and pressure via plasma-assisted ammonia synthesis. However, the efficiency of plasma-assisted ammonia synthesis alone is not high because the strength of the NN bond (NN bond = 946 kJ/mol) is much greater than that of the NH bond (NH bond = 389 kJ/mol) at room temperature. Therefore, the choice of proper catalysts to improve the selectivity of the reaction products is also a hot topic of research.

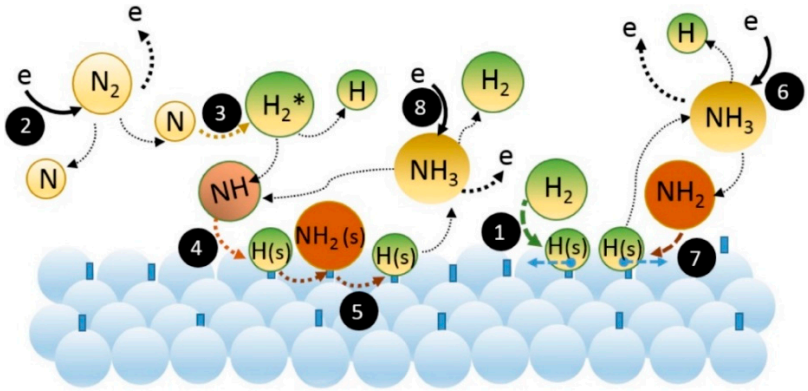

Figure 2. The main reaction process of plasma ammonia synthesis [25].

An efficient catalyst should exhibit not only strong adsorption of reactants but also low dissociation energy of products, which is contradictory to the catalyst itself. However, it is possible to modulate the bonding strength of N_2 and catalyst by elaborate design of alloy catalysts based on the surface bonding energy between metal atoms and N atoms. Xie et al. [26] prepared a high-entropy alloy (HEA) containing five common metallic elements that became saturated at 600 °C (with 100% conversion), and it was much more effective in catalysis than the noble metal Ru (with 73% conversion).

3. Limitations of Ammonia Fuel in ICEs

3.1. Ignition Energy

The minimum ignition energy (MIE) is typically defined as the minimum energy required to ignite the combustible gas [27], and a lower MIE indicates that a stable fire nucleus can be formed more easily in the early stages of combustion. Although ammonia has a high hydrogen content, pure ammonia combustion is inherently difficult to ignite. An ignition energy of 2.8 J is still required in spite of mixing with hydrogen fuel under a modified ignition system, which is two orders of magnitude higher than hydrocarbon fuel and four orders of magnitude higher than hydrogen [28]. Xin et al. [29] performed experimental studies on combustion and emission properties of a hydrogen/ammonia-fueled engine at part-load operating conditions. As illustrated in Figure 3a,b, the addition of ammonia changed the combustion characteristics by prolonging ignition delay times (duration of CA0-10) and flame development periods (duration of CA10-90) due to its higher ignition energy. Meanwhile, the combustion phase was still controllable by modulation of ignition timing for improved indicated thermal efficiency (ITE) and acceptable NOx emission.

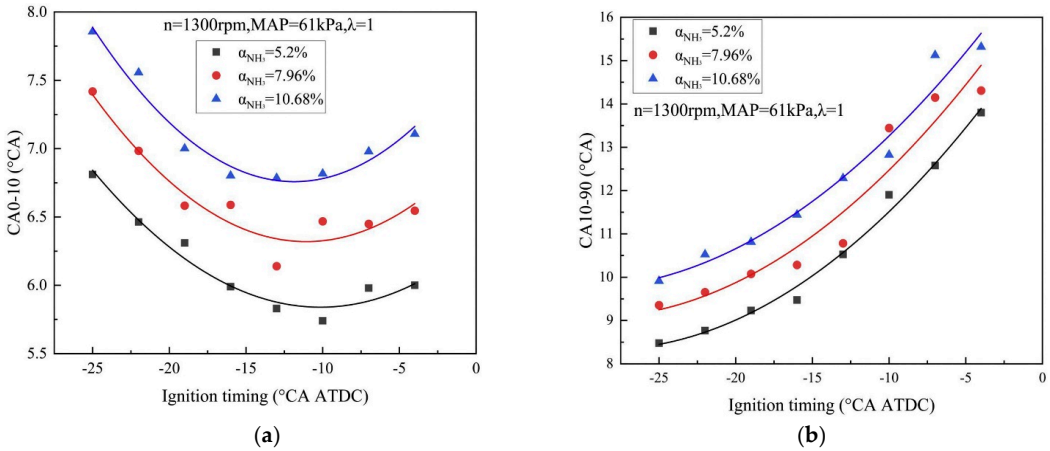

(**a**) (**b**)

Figure 3. Combustion durations versus ignition timing at different ammonia levels [29]. (**a**) duration of CA0-10 for varied addition of ammonia (**b**) duration of CA10-90 for varied addition of ammonia.

3.2. Flame Speed

The primary limitation on the practical usage of ammonia as an engine fuel is the relatively slow flame speeds. The laminar burning velocity (LBV or Su) is an important parameter to characterize the premixed combustion process. Investigations on accelerating NH_3 efficient combustion with fuel additives have attracted the interest of many researchers. Numerical studies on the performance of premixed combustion of NH_3/H_2/air mixtures was conducted by Wang et al. [28] using Cantera open-source code. It was shown that the properties of NH_3/H_2/air mixture combustion could be comparable to that of hydrocarbon fuels under engine-relevant conditions; therefore, a high compression ratio is tolerable because of the excellent knock-resistance ability of the NH_3/H_2 mixture. In addition, the increase in Su with H_2 addition contributes to facilitated diffusion, intensified reactivity, and increased flame temperature. At a compression ratio of 10, Su is observably improved with more H_2 added. However, for the stoichiometric combustion of NH_3/H_2, there still needs to be a 39% hydrogen doping ratio to reach a comparable Su level as CH_4 combustion.

Lhuillier et al. [30] found the same phenomenon when studying ammonia blends under engine-relevant turbulent conditions: enrichment of hydrogen in ammonia leads to an earlier, more intense heat release. To figure out the effects of additives such as H_2, CO and CH_4 on the Su of ammonia blend combustion, Han et al. [31] proposed normalized enhancement parameters for quantitative analysis of the enhancement level. It was concluded that the effects of H_2 enhancement were exponential, while non-monotonic with CO and almost linear with CH_4 at mixing ratios greater than 0.2. Very low Su is constrained with pure CO/air combustion since almost no H or OH radical is accumulated during combustion, as shown in Figure 4, but when blended with moderate CO in NH_3, a rapid increase in Su is achieved by decomposed H and OH radicals. The trends of Su almost coincided with the curves of the maximum H molar fraction, which implied the effect of H radicals on Su was dominant. Similar findings with concentration of H and OH radicals were also reported in the flame combustion of ammonia/methane/air [32].

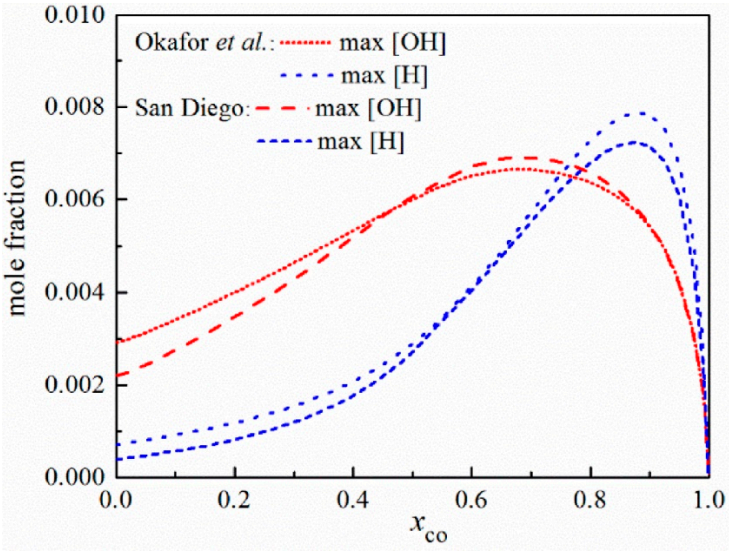

Figure 4. Maximum molar fraction of H and OH radicals of stoichiometric NH_3/CO/air flame [31].

3.3. NOx and Unburned NH_3 Emissions

The use of ammonia fuels is effective in reducing hydrocarbon emissions, but relatively it also increases the content of NOx and unburned NH_3 in exhaust. Representing significant progress in microscopic combustion kinetic reactions, chemical kinetic mechanisms are widely used to understand how quickly or slowly chemical reactions occur in nature. Numerous robust and concise chemical kinetic mechanisms have been proposed for ammonia oxidation under a wide range of conditions after verification of combustion characteristics and NOx emission. Since ammonia chemistry is less complex than that of hydrocarbons,

the most recent ammonia oxidation mechanisms in different studies are generally fairly compatible. However, the differences are largely limited to the choice of rate constants or branching ratios for specific elementary reaction groups in varied application circumstances [33]. It is concluded that NO generation in burning lean ammonia depends heavily on OH radicals and HNO relative reactions, but under rich-ammonia combustion, rich H radicals promote formation of NH_x radicals [34]. However, as concluded by Li et al. [35], development of an accurate mechanism to model ammonia-based flame is urgently necessary. Apart from NOx emission, the carbon capture from low-carbon fuel-assisted ammonia flame is still worth studying.

Wang et al. [28] studied the performance of premixed hydrogen–ammonia combustion by simulations. The integrated rate of production (ROP) of NO and the species molar fraction with varied hydrogen molar fraction α are displayed in Figure 5. NO was considered the main source of NOx and two competitive mechanisms of NO production were analyzed: on the one hand, as more H content involved, the flame temperature and concentrations of reactive O/H radical were both increased, leading to a growth in NO generation as well as NH_3 conversion; on the other hand, the decrease in the reactant NH_3 suppressed the NO-related reaction rates in turn. Unlike fuel NO, which was formed with NH_3, the hot NO was more likely to be formed with the increasing of flame temperature caused by O/H radicals. Moreover, NO_2 was rapidly generated by conversion from NO in the flame region, then reconverted back to NO in the post-flame region via $NO_2 + O \rightarrow NO + O_2$, which finally reduced the total amount of NO_2 [36,37]. Jin et al. [38] investigated the effect of different ammonia-to-energy ratios (AER) on the combustion and emission characteristic of an ammonia–diesel dual-fuel engine. Compared to pure diesel engines, the NO emission was decreased instead with increasing AER because of the denitrification of amine, forming more stable N_2 via reduction reaction. However, the incomplete combustion of NH_3 was increased significantly due to the low combustion temperature.

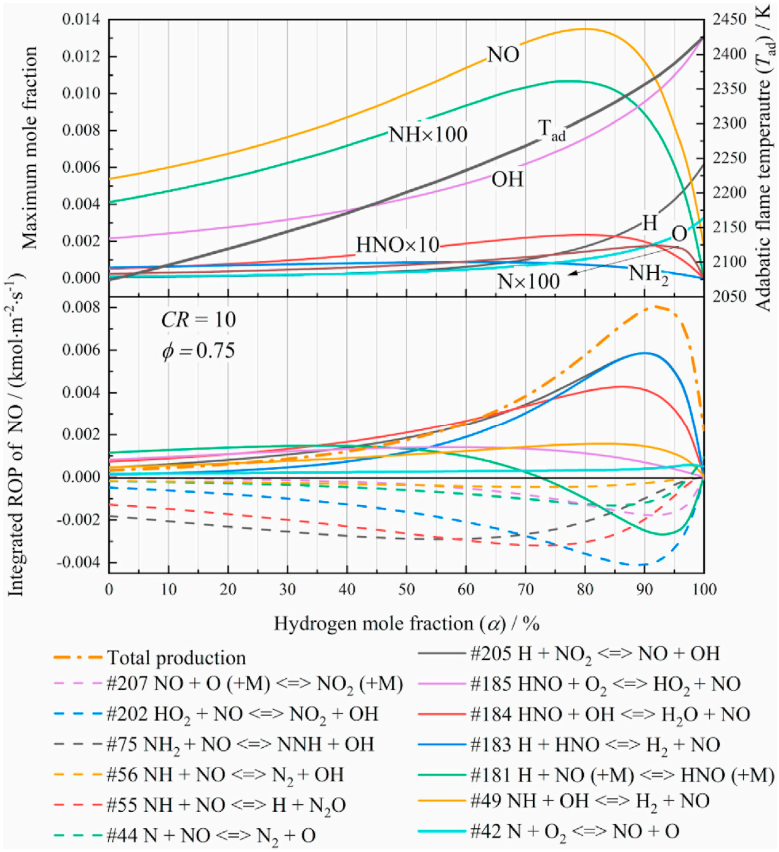

Figure 5. Temperature distribution and integrated production rate such as NO varies with α, φ = 0.75, CR = 10 [28].

As mentioned above, obstacles to the further development of ammonia-fueled engines are large minimum ignition energy, lower flame speed, and more NOx emission with unburned NH_3. However, some new technologies expanded on the next chapter are expected to overcome the difficulties.

4. Current Technologies of Ammonia-Fueled Engines

4.1. Oxygen-Enriched Combustion

It has been confirmed that oxygen-enriched combustion has the ability to lower fuel ignition points, speed up reactions, widen combustion limits and raise flame temperature. Therefore, some scholars studied the combustion characteristics of ammonia under oxygen-enriched conditions. For internal combustion engines, the advantages of oxygen-enriched technology solve the problems of further oxidation of CO and unburned hydrocarbons, but bring higher NOx emissions [39–44]. In order to overcome the shortcomings caused by oxygen enrichment, Liang et al. [45] applied an emulsification technique to diesel, which made the fuel unstable and then disperse throughout the combustion chamber after micro-explosion during the compression stroke in the engine. As a result, the combination of water diesel emulsion and oxygen-enriched combustion reduced the combustion temperature in the cylinder, thus leading to less NOx emission, while the output power of the engine was lower than the normal level. Karimi et al. [46] investigated the effects of oxygen enrichment on the combustion and emission characteristics of a hydrogen–diesel dual fuel (HDDF) engine under low load. Compared with traditional HDDF engines, the oxygen-enriched conditions improved the characteristics of low combustion temperature and laminar flame speed under low load, thus reducing ignition delay. However, more NOx was emitted than a diesel-only engine, but this could be reduced through the EGR technique. Since ammonia engines are not widespread, most of the research on ammonia has been on basic combustion characteristics. An experimental and kinetic modeling investigation on the laminar flame propagation of ammonia was conducted by Mei et al. [47] under oxygen-enrichment conditions. It was found the laminar burning velocity increased with the increasing oxygen content in both experimental and numerical studies, which was driven by the enriched concentrations of key radicals H, OH and NH_2. However, the oxygen enrichment also caused more NOx emissions in turn. Wang [3] investigated the basic characteristics of ammonia fuel in a constant-volume bomb, and the modeling-predicted laminar burning velocities by Cantera code under oxygen enrichment are given in Figure 6. The laminar flame velocity in the ammonia-burning system increased first and then declined as the equivalence ratio changed from 0.6 to 1.5, predicted by varied mechanisms. The greater the oxygen enrichment, the faster the laminar flow flame speed. Meanwhile, there was an interesting phenomenon: the equivalent ratio corresponding to the maximum laminar flame velocity moved towards the lean combustion side with increasing oxygen enrichment Ω. Similar findings were discovered for NOx emissions. As a result, when considering oxygen enrichment to assist ammonia combustion, NOx emissions should be given special attention.

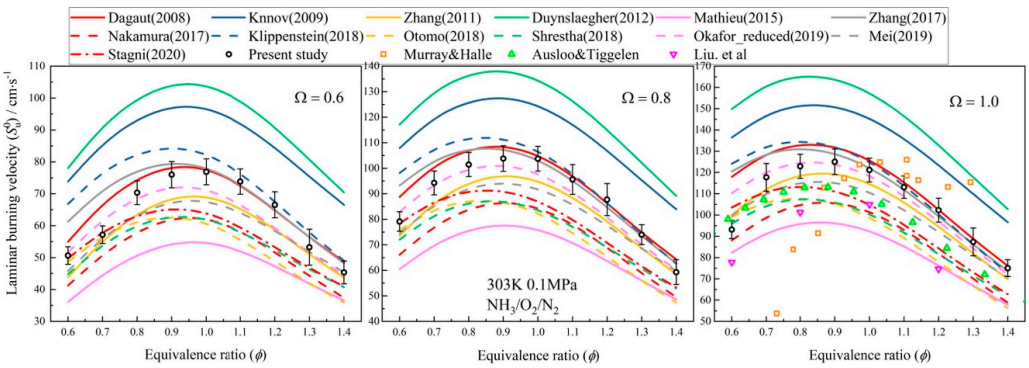

Figure 6. Comparison of predicted laminar flame velocity of ammonia with low oxygen-rich concentration [3].

4.2. Ammonia–Hydrogen Mixed Combustion

To improve the combustion characteristics of ammonia, it is effective to blend hydrogen with ammonia fuel because hydrogen laminar combustion is faster while having a wider combustion limit compared with ammonia. Differently from dual-fuel combustion or oxygen-enriched combustion, addition of hydrogen derived from partially cracked ammonia typically improves the combustion properties under the conditions of high temperature, high pressure and suitable catalyst. A basic investigation on ammonia decomposition was conducted by Ganley et al. [48], who evaluated the activity of metal catalysts: Ru > Ni > Rh > Co > Ir > Fe > Pt > Cr > Pd > Cu >> Te, Se, Pb. Comptti et al. [49] developed a hydrogen generation system (HGS) for ammonia–hydrogen-fueled internal combustion engines using a commercial ruthenium-based catalyst named ACTA 10010. The HGS heated by exhausted combustion gases performed well in hydrogen production, engine brake thermal efficiency and net heat release, but poorly for NOx emissions. Similar results can be found in the work by Ryu et al. [50], and it is emphasized that only a low ammonia flow rate would improve combustion performance.

Apart from dissociating NH_3 in situ from hydrogen, another method of preparing an NH_3/H_2 mixture is to inject hydrogen and ammonia into the intake manifold in the gaseous phase separately [51]. Zhang et al. [52] conducted a numerical investigation on the effects of hydrogen-rich reformate addition on the combustion and emission characteristics of an ammonia engine. It was found that the in-cylinder pressure and heat release rate increased almost linearly with the increasing reformate blending ratio (R_{re}) in stoichiometric cases. This is because more H and OH radicals were generated by the reaction $H_2 + O \rightarrow H + OH$ and the production would promote the consumption of NH_3. The increase in the combustion temperature resulting from greater R_{re} also reduced the emission of unburned NH_3 and N_2O, but too high a reforming ratio would appear undesirable, and thus they recommended a ratio of 7.5–10% near stoichiometry. Li et al. [53] investigated the effects of an ammonia–hydrogen mixture on combustion stability in a single-cylinder, four-value optical SI engine. The results showed that compared with a pure ammonia engine, the misfire phenomenon could be avoided by 5% hydrogen addition, 7.5% was the best thermal efficiency, and more than 20% would lead to unstable combustion. This is because a small amount of hydrogen would increase the combustion temperature in the cylinder and accelerate the ammonia oxidation, while further increasing the hydrogen content would cause heat loss, resulting in a decrease in the indicated thermal efficiency.

To understand the effect of cracking ratio on ammonia combustion, Mei et al. [54] performed both experimental and kinetic numerical investigations on laminar flame propagation of partially cracked NH_3/air mixtures. It was reported the laminar flame speed of the mixture was improved as the cracking ratio increased. The combustion was comparable to methane combustion with a cracking ratio of 40% at atmospheric pressure. Wang [3] investigated the variations in laminar flame speeds with different ammonia oxidation mechanisms at low hydrogen-doping ratios under ambient temperature and pressure conditions. It was found that the laminar flame speed increased significantly with increasing hydrogen-doping ratio α in both simulation and available experiments, since more O/H radicals produced by hydrogen accelerated the oxidation reaction of ammonia. Nevertheless, more NO was formed because NH radicals converted directly to NO without HNO oxidation and the conversion of NO to N_2O would be reduced by higher flame temperature.

Lhuiller et al. [55] investigated the behaviors of an ammonia-fueled engine at different H_2 concentrations, equivalence ratios and boosted pressures. It was found that an engine with high hydrogen concentrations performed well under lean combustion conditions, since the addition of H_2 promoted ignition and combustion stability. Wang et al. [56] studied the combustion characteristics of a NH_3/H_2 mixture with high hydrogen doping ratio (30%) in a medium-speed marine engine. As the equivalence ratio increased, it failed to ignite unless the initial intake temperature and pressure increased, but this limitation could be overcome when moderate proportion of hydrogen doping was added, for example, the peak flame temperature exceeded 2150 K at a 40% hydrogen doping ratio. However, if more hydrogen

is required to achieve the assisted-ignition effect [57], it brings new challenges to ensure safe engine operation, since a large amount of additional hydrogen needs to be stored for fuel supply. In general, dual-fuel compression ignition engine operation with ammonia is dependent on the cetane number of pilot fuel and its injection strategies. The concerns of high unburned ammonia and NOx emissions because of the fuel-bound nitrogen are expected to be mitigated by an aftertreatment system. Thus, ammonia can be positively seen as a feasible solution as an alternative fuel for ICEs, without significant engine refit.

5. Plasma-Assisted Combustion Technology

5.1. Principle of Plasma-Assisted Combustion

Plasma is the fourth kind of matter distinguished from solid, liquid and gas, consisting of a large number of charged particles and neutral particles, which are electrically neutral. It can be classified into thermal equilibrium plasma and nonequilibrium plasma. Thermal or equilibrium plasmas are characterized by high energy density and equality between the temperature of heavy particles and electrons, while conversely a nonequilibrium plasma characteristic is a lower-pressure plasma with low ion and neutral temperatures, as shown in Figure 7. Nonequilibrium plasma plays a similar role to a catalyst to activate ambient gas molecules at room temperature and pressure through colliding and dissociating chemical bonding with the help of high-energy electrons [58,59]. Plasma generation methods commonly used are dielectric barrier discharge (DBD), atmospheric pressure plasma jet (APPJ) and sliding arc discharge plasma (GAD), while pulsed power is the most commonly used excitation power source for atmospheric low-temperature plasma [60].

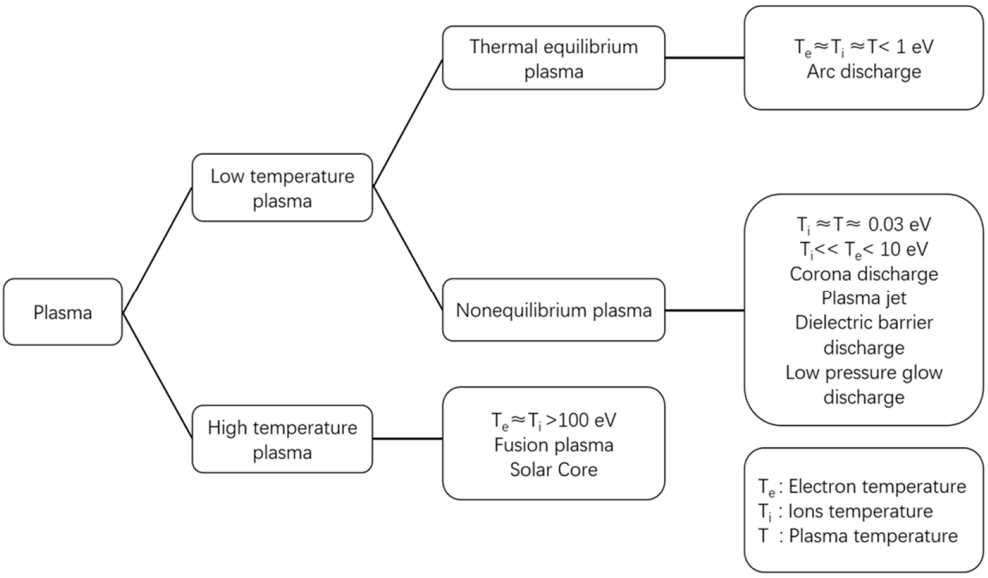

Figure 7. Plasma classification.

The enhancement of plasma-assisted combustion is achieved mainly through three pathways, as illustrated in Figure 8: thermodynamic effects, kinetic effects and transport [61]. Thermodynamically, the increase in overall gas and electron temperatures is ascribed to the energy conversion of the plasma discharge and the exotherm of chemical reactions, thus further accelerating the reactions. Kinetically, a large number of high-energy electrons and active particles involved in plasma not only facilitate chemical reactions due to the reduced activation energy but also introduce new branched reactions in the original system. For transport, plasma discharge will form ionic wind, which can accelerate the mixing process of reaction gases.

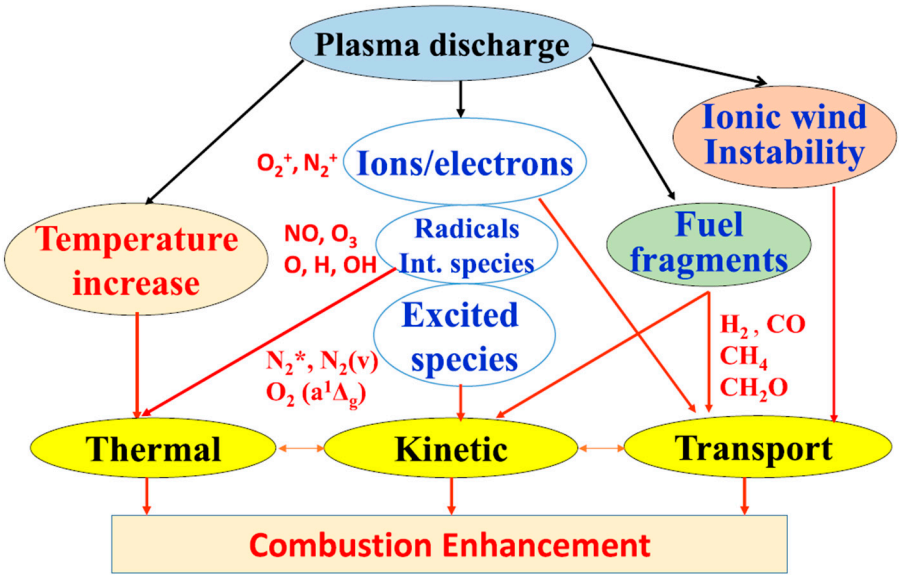

Figure 8. Principle of plasma-assisted combustion [61].

As mentioned, plasma-assisted combustion involves complicated plasma dynamics and combustion kinetics, so it is difficult to decouple the plasma effect and thermal effect from the perspective of conventional experiments due to cross-disciplinary complexity. Although it has been verified that plasma can play a significant role in enhancing combustion, modulating emissions and fuel reforming, the underlying mechanisms are a worthy ongoing topic in different application scenarios.

5.2. PAC Ignition Enhancement

It was found plasma-assisted combustion (PAC) can overcome the flame extinction limit and that PAC ignition enables lower-temperature combustion in contrast to high-temperature ignition, while it must follow the ignition S-curves in conventional ignition process, as shown in Figure 9 [61]. For internal combustion engines, plasma generated by different types of discharge such as microwave [62], radio frequency [63], laser ignition [64] and nanosecond pulses (NRP) [65,66], has been used to assist ignition and combustion. Among these, NRP has a significant advantage applied in low-energy ignition. To clarify the cumulative effect of repetitive NRP pulse number on the PAC, Barleon et al. [67] investigated the ignition of a premixed methane–air mixture by NPR in pin-pin configuration. The conclusion was that there was less total energy required as the pulse frequency increased. Compared with traditional spark ignition, Cathey et al. [65] found that it caused shorter ignition delay, higher peak pressure and greater net heat release in a single-cylinder gasoline engine through NRP. In fact, the expected minimum ignition energy is controlled by the minimum flame radius [61], which has a strong relationship to the Lewis number of the mixture, the fuel reactivity (activation energy) and the flame thickness. Therefore, the reduced ignition delay and lowered ignition energy by PCA were to a great extent due to the increase in the diversity of the reaction system (reduced Lewis number) and the decrease in activation energy.

The reduced electric field E/N is the most significant parameter to control the distribution of energy deposited to the different excitation modes and then generate active particles. Research to figure out the best reduced electric field to minimize the ignition time of CH_4/Air/He mixture was conducted by Mao et al. [68] using a combination of nanosecond pulses and DC discharges. In their study, a DC electric field of 5 Td minimized the time used for ignition, as shown in Figure 10, and it was revealed that the low-DC electric field promoted the excitation of CH_4(v) and O_2(v) effectively, as well as O_2(a1Δg), which played a positive role in ignition enhancement through pathway flux analysis.

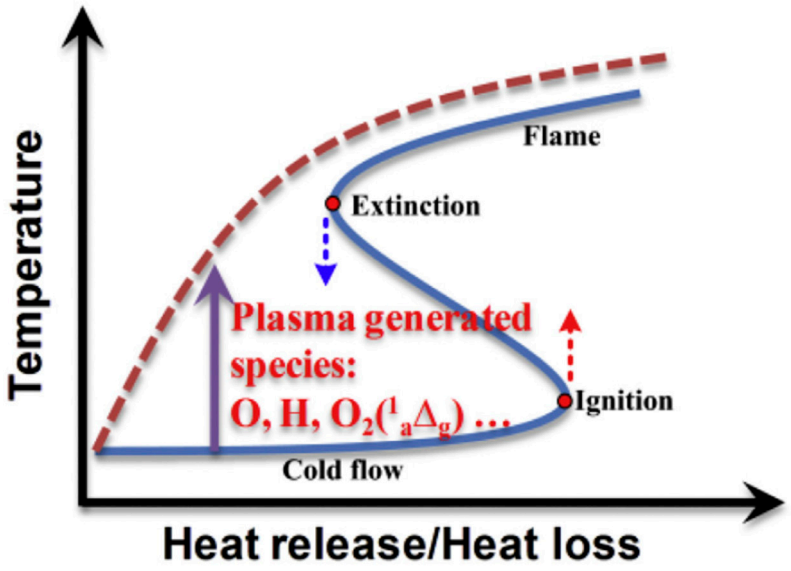

Figure 9. Schematic diagram of the plasma-assisted transition from the classical ignition and extinction S-curve (blue solid line) to the monotonic stretching S-curve (red dashed line) [61].

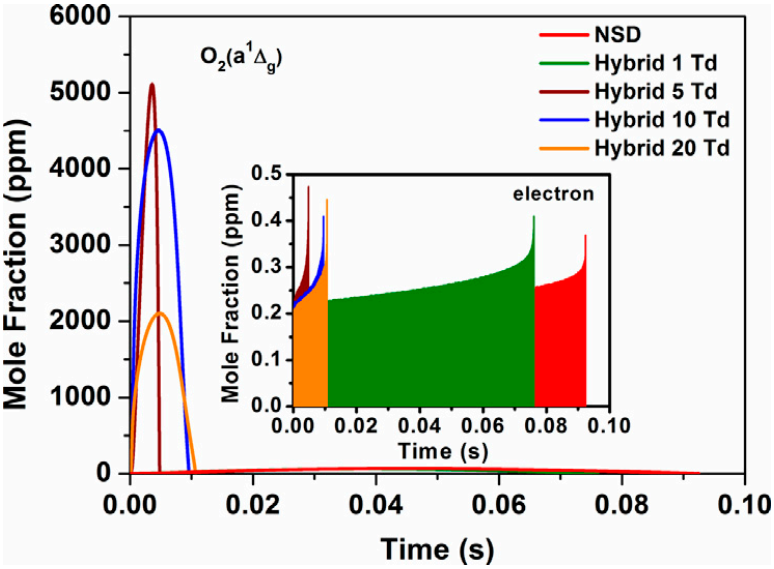

Figure 10. Time evolution of O_2(a1Δg) for NSD and mixed discharges with different DC field strengths at 900 K [68].

Furthermore, the time scale of plasma kinetics is within the order of nanoseconds, while the combustion kinetics fall in ranges from micro- to milliseconds [61], as illustrated in Figure 11. Therefore, the PAC process is the coupling of long-life plasma species with active radicals from fuel pyrolysis via energy transfer and kinetic interaction. From this point of view, the bridge linking fast plasma kinetics and combustion kinetics is critical to fully explore the PAC principles. This motivates the development of an efficient numerical model for multi-timescale PAC. Recently, the zero-dimensional plasma kinetic solver ZDplaskin incorporated with combustion kinetic solver CHEMKIN has been the most widely used numerical tool for PAC. ZDplaskin integrated with Boltzmann equation solver (BOLSIG+) is used to predict time evolution of neural radical and active species. Rate coefficients are formulated based on the incident energy by plasma discharges and collisional cross sections data of electron-associated reaction in LXCat format. Many studies have employed the ZDplaskin-CHEMKIN solver to study flame stability, contemplating the effects of plasma discharges on the flame propagation characteristics and ignition delay

times [68,69]. However, there remain challenges in developing plasma kinetic mechanisms accommodating low-temperature and high-pressure conditions. At present, 2-D and 3-D numerical tools are not available for PAC modeling.

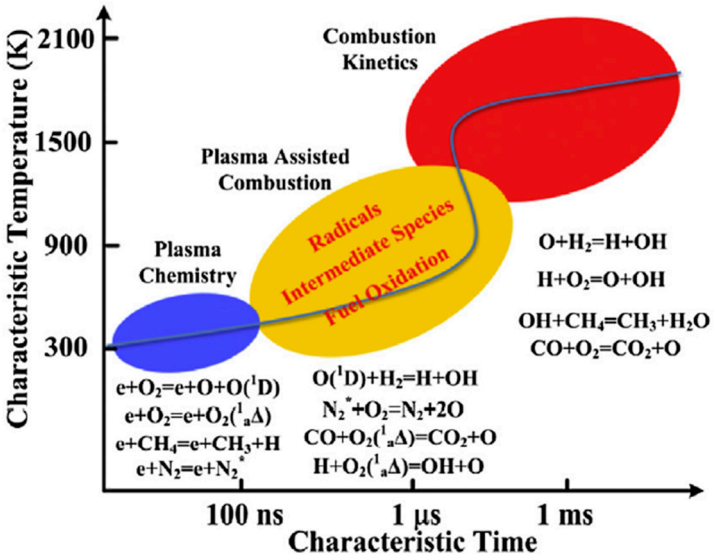

Figure 11. Schematic of timescales for PAC kinetics [61].

The dilution of different types of inert gases also affects electron energy distribution function in plasma, thus influencing the mixture combustion reactivity. A numerical investigation on the effects of methane pyrolysis with different diluents (N_2/Ar/He) was conducted by Mao et al. [70] using the zero-dimensional solver ZDPlasKin coupled with CHEMKIN. The results indicated that the quenching of electronic excited states and relaxation of the vibrational state contributed greatly to the pyrolysis of CH_4, for which the addition of N_2 as diluent performed best. As a result, it is concluded the excited states of equilibrium gases play a dominant role in physicochemical mechanisms and fuel oxidation efficiency through collisional quenching reactions. Similar findings were reported by Snoeckx et al. [71].

The commercial applications of plasma on ICEs are still immature, but many investigations are being carried out. Hwang et al. [72] developed a new microwave-assisted plasma ignition system and applied it to a direct injection gasoline engine. The new ignition system has a shorter ignition delay and a more advanced combustion stage than conventional spark ignition systems. It also broadened the thin combustion limit since it can form a larger fire nucleus by providing abundant reactive radicals over a larger area. A laser-induced plasma (LIP) ignition system has been evaluated to assist the ignition of a diesel–gasoline mixture in a CI engine by José et al. [73]. It was reported that the LIP ignition system can effectively solve the problem of automatic ignition of mixed fuels under different operations, and in addition, the variable height ignition technology improved combustion efficiency and reduced hydrocarbon emissions. L. et al. [74] investigated the ignition behavior of a methane–air mixture in an optically equipped setup consisting of a double chamber under repeated pulse discharge (NRPD). It showed that NRPD has a higher ignition success rate and average flame front propagation compared to standard inductive ignition. It can achieve lean combustion by adjusting the energy and number of pulses, but it did not work after inflammation.

6. Plasma-Assisted Ammonia Ignition

As mentioned above, addition of hydrogen derived from partially cracked ammonia typically improves the combustion properties. Direct decomposition of ammonia to hydrogen is a typical endothermic reaction with an enthalpy change of 91.2 kJ/mol. The decomposition of ammonia is able to be achieved at high temperature in the presence

of a classic selective catalyst. Nevertheless, plasma catalysis is a promising approach to decompose ammonia at low temperature (<450 °C), but with a relatively high conversion rate. The synergistic effect of plasma and catalyst refers to the truth that it affects the catalytic process more than the sum of plasma and catalyst alone [75]. Although plasma catalytic ammonia synthesis is well understood, plasma catalytic ammonia decomposition still needs further study, and there is no commercial application available so far. Research on plasma catalytic ammonia decomposition has been centered on experiments, most of which have focused on designing high-efficient catalyst to improve hydrogen conversion. Wang et al. [76] measured the effect of DBD plasma synergism with Fe-based catalysts on ammonia decomposition efficiency through optical diagnostics and isotope scanning techniques. It was revealed the excited-state NH_3* and NH* played an important role in N atoms desorption, thus influencing conversion efficiency as the reaction temperature reduced by 100–140 °C. In their subsequent study [77], it was found the plasma promoted the chemisorption of NH_3*, leading to increased conversion by nearly 40% at 550 °C. The underlying physicochemical mechanisms of plasma catalytic kinetics should be further explored in depth to facilitate its practical usage in on-site hydrogen generation.

A number of simulation studies were carried out by using the kinetic model under wide conditions of temperatures ranging from 600 to 1500 K, and the characteristics of plasma-assisted ammonia combustion were predicted with varying pulsation frequencies and pulse numbers. Faingold and Lefkowitz [78] employed ZDplaskin-CHEMKIN with an assembled kinetic model for the oxidation of ammonia/oxygen/helium to perform pulse repetition frequencies (PRFs) on ignition delay times (IDTs). It was found IDTs could be reduced by 40–60%, as shown in Figure 12, under a moderate number of pulses. Higher PRFs promote an expanding radical pool, whereas lower PRFs favor the radical recombination between pulses.

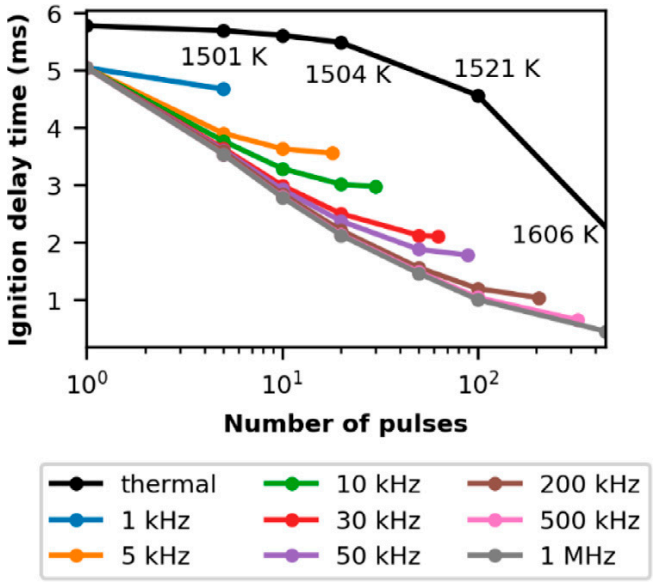

Figure 12. IDTs for different PRFs and number of pulses [78].

A series of experiments on plasma-assisted ammonia combustion were carried out because of the great advantages of plasma-assisted combustion as mentioned before. Lin et al. [79] studied the performance of plasma-assisted combustion via a new gliding arc plasma (GAP) generator combined with a cyclonic burner. The operation map of ammonia combustion flames with the GAP on or off is displayed in Figure 13, in which the ammonia combustion limitation was widened under both air and ammonia GAP. However, if the equivalence ratio exceeded 2.2 under a high air flow rate, the ammonia combustion flame would become unstable. Furthermore, the physicochemical mechanisms of discharged air and ammonia worked differently. The particles (OH*, H* and O*) played a dominant

role in the dehydrogenation reaction of ammonia through kinetic mechanisms for the former (air medium) while the latter (ammonia medium) improved the combustion limit by the hydrogen produced from ammonia directly. A similar investigation on ammonia combustion was conducted by Choe et al. [80] using a nanosecond high-pressure pulse generator. It was concluded that plasma was able to extend the lean blowoff limits of ammonia flames and reduce NOx emissions simultaneously, but further research needs to be focused on the interaction between plasma dynamics and combustion kinetics.

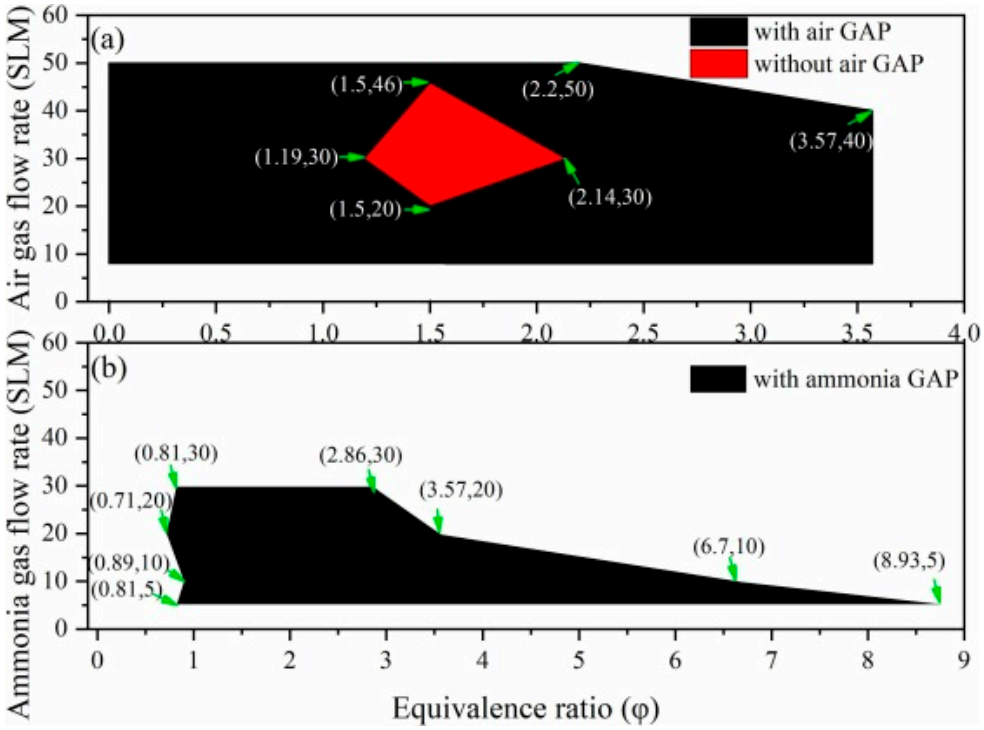

Figure 13. An operation map of ammonia combustion flames under the following conditions: (**a**) air GAP working on/off and (**b**) ammonia GAP working on.

Plasma-assisted ammonia combustion has great capacity for shortening ignition delay timing and extending combustible ranges while reducing NOx emissions. It will definitely promote the use of ammonia in engines. This has attracted lots of attention from scholars dedicated to figuring out the underlying physicochemical mechanisms via theoretical analysis and numerical simulation. Taneja et al. [81] found that PAC achieved the fastest ignition in a lean fuel mixture because of the accumulation of OH radicals through the reactivity-inhibiting reactions between plasma pulses, while an inversely proportional impact on ignition delay times was exhibited on plasma pulse frequency and energy density deposited. Moreover, the reforming of ammonia to nitrogen resulted in lower production of NOx with plasma. Another similar investigation also discovered PAC changed the conventional ignition and extinction characteristics, and the S-shaped curves were replaced by the monotonic and stretched ignition curves, which made low-temperature ignition possible [78]. Shahsavar et al. [82] figured out the most effective range of a reduced electric field on ammonia equivalent ratio combustion: 250–400 Td. This greatly promoted ignition time by increasing the reduced electric field in the early stage. With a more reduced electric field, a large fraction of the energy in the plasma system would be utilized in the ionization reactions of the diluent, thus neutralizing the effective excitations of fuel and oxidizer species, as shown in Figure 14.

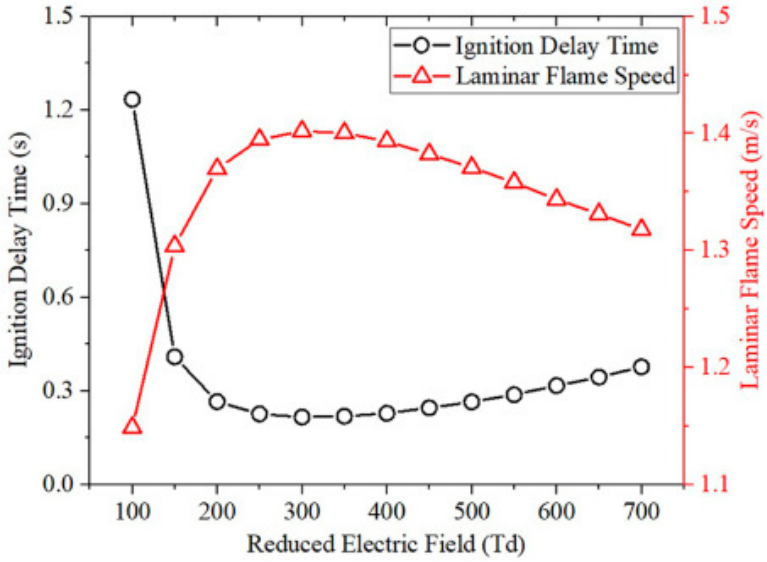

Figure 14. Effects of reduced electric field on ignition delay times and laminar flame velocities for plasma-assisted $NH_3/O_2/N_2$ combustion [82].

Finally, when projecting the adoption of plasma as an encouraging approach to boost ammonia decomposition and ignition, this review summarizes the latest innovations in the field of plasma catalysis and PAC, including progress in both numerical models and experimental studies. Great interest in improving ignition delay timing, increasing flame speed, and extending flammability limits while reducing NOx emissions will promote fast application in practical ICEs.

7. Conclusions

The outlook of independence from conventional fossil fuels is decarbonization in the automotive, marine and power generation sectors. Towards this goal, running with carbon-free fuel such as ammonia in ICEs is drawing more attention in research activities. Currently, ammonia can be ignited with diesel or any other high-reactivity fuel in dual-fuel mode, especially in marine engines and heavy-duty engines. Moreover, the addition of hydrogen is able to be derived from partially cracked ammonia with suitable catalyst in situ. However, the optimal hydrogen ratio in ammonia–hydrogen mixed combustion should not exceed 10%, considering thermal efficiency and combustion stability. A promising technology of plasma-assisted combustion to overcome the bottleneck of ammonia limits has attracted positive interest. The fundamental mechanisms of possible technical advances emerging in assisted combustion of ammonia are reviewed in this study.

(1) The laminar burning velocity of ammonia combustion increased with the increasing oxygen content, driven by the enriched concentrations of key radicals H, OH and NH_2. The maximum laminar flame velocity corresponds to equivalent ratio combustion, but the maximum NOx emissions moved towards lean combustion with increased oxygen enrichment.

(2) Investigations of ammonia-fueled engines have been widely carried out with varied additions of hydrogen, but modulations of inlet temperature and pressure are still necessary, especially for lean combustion. If more hydrogen is needed, it must be a new challenge to ensure operation safety with hydrogen supply.

(3) Plasma-assisted combustion enables lower-temperature combustion and has ability to overcome the flame extinction limit while reducing NOx emissions, due to the increase in diversity via active particles in the reaction system and the decrease in activation energy. The underlying physicochemical mechanisms of plasma-assisted ammonia combustion are rarely reported. The accumulation of OH radicals through reactivity-inhibiting reactions in lean fuel combustion could be stimulated through thermodynamic and kinetic effects via proper plasma generator configuration.

Funding: This research was funded by Open Funds of State Key Laboratory of Engine Reliability grant number [skler-202109], and Shandong Provincial Natural Science Foundation grant number [2022HWYQ-061, ZR2021ME212].

Data Availability Statement: Not applicable.

Conflicts of Interest: The authors declare no conflict of interest.

References

1. Dawood, F.; Anda, M.; Shafiullah, G.M. Hydrogen production for energy: An overview. *Int. J. Hydrogen Energy* **2020**, *45*, 3847–3869. [CrossRef]
2. Gorky, F.; Lucero, J.M.; Crawford, J.M.; Blake, B.A.; Guthrie, S.R.; Carreon, M.A.; Carreon, M.L. Insights on cold plasma ammonia synthesis and decomposition using alkaline earth metal-based perovskites. *Catal. Sci. Technol.* **2021**, *11*, 5109–5118. [CrossRef]
3. Wang, D.; Ji, C.; Wang, Z.; Wang, S.; Zhang, T.; Yang, J. Measurement of oxy-ammonia laminar burning velocity at normal and elevated temperatures. *Fuel* **2020**, *279*, 118425. [CrossRef]
4. Bartels, J.R. A Feasibility Study of Implementing an Ammonia Economy. Master's Thesis, Iowa State University, Ames, IA, USA, 2008.
5. Giddey, S.; Badwal, S.P.S.; Munnings, C.; Dolan, M. Ammonia as a renewable energy transportation media. *ACS Sustain. Chem. Eng.* **2017**, *5*, 10231–10239. [CrossRef]
6. Smith, C.; Hill, A.K.; Torrente-Murciano, L. Current and future role of Haber–Bosch ammonia in a carbon-free energy landscape. *Energy Environ. Sci.* **2020**, *13*, 331–344. [CrossRef]
7. Hasan, M.H.; Mahlia, T.M.I.; Mofijur, M.; Fattah, I.M.R.; Handayani, F.; Ong, H.C.; Silitonga, A.S. A comprehensive review on the recent development of ammonia as a renewable energy carrier. *Energies* **2021**, *14*, 3732. [CrossRef]
8. Schiffer, Z.J.; Manthiram, K. Electrification and decarbonization of the chemical industry. *Joule* **2017**, *1*, 10–14. [CrossRef]
9. Kyriakou, V.; Garagounis, I.; Vourros, A.; Vasileiou, E.; Stoukides, M. An electrochemical Haber-Bosch process. *Joule* **2020**, *4*, 142–158. [CrossRef]
10. Elmøe, T.D.; Sørensen, R.Z.; Quaade, U.; Christensen, C.H.; Nørskov, J.K.; Johannessen, T. A high-density ammonia storage/delivery system based on $Mg(NH_3)_6Cl_2$ for SCR–DeNOx in vehicles. *Chem. Eng. Sci.* **2006**, *61*, 2618–2625. [CrossRef]
11. Rouwenhorst, K.H.R.; Elishav, O.; Mosevitzky Lis, B.; Grader, G.S.; Mounaïm-Rousselle, C.; Roldan, A.; Valera-Medina, A. Future Trends. In *Techno-Economic Challenges of Green Ammonia as an Energy Vector*; Elsevier: Amsterdam, The Netherlands, 2021; pp. 303–319.
12. Herbinet, O.; Bartocci, P.; Dana, A.G. On the use of ammonia as a fuel—A perspective. *Fuel Commun.* **2022**, *11*, 100064. [CrossRef]
13. Dimitriou, P.; Javaid, R. A review of ammonia as a compression ignition engine fuel. *Int. J. Hydrogen Energy* **2020**, *45*, 7098–7118. [CrossRef]
14. Bicer, Y.; Dincer, I. Life cycle assessment of ammonia utilization in city transportation and power generation. *J. Clean. Prod.* **2018**, *170*, 1594–1601. [CrossRef]
15. Brown, T. UK Department of Transport Recommends Launch of Ammonia/Hydrogen Powered Vessels within 5–15 Years [EB/OL]. Ammonia Energy. 2019. Available online: https://www.ammoniaenergy.org/articles/uk-department-of-transport-recommends-launch-of-ammonia-hydrogen-powered-vessels-within-5-15-years/ (accessed on 26 June 2023).
16. Valera-Medina, A.; Amer-Hatem, F.; Azad, A.K.; Dedoussi, I.C.; de Joannon, M.; Fernandes, R.X.; Glarborg, P.; Hashemi, H.; He, X.; Mashruk, S.; et al. Review on ammonia as a potential fuel: From synthesis to economics. *Energy Fuels* **2021**, *35*, 6964–7029. [CrossRef]
17. Dimitriou, P.; Tsujimura, T. A review of hydrogen as a compression ignition engine fuel. *Int. J. Hydrogen Energy* **2017**, *42*, 24470–24486. [CrossRef]
18. Cardoso, J.S.; Silva, V.; Rocha, R.C.; Hall, M.J.; Costa, M.; Eusébio, D. Ammonia as an energy vector: Current and future prospects for low-carbon fuel applications in internal combustion engines. *J. Clean. Prod.* **2021**, *296*, 126562. [CrossRef]
19. Juangsa, F.B.; Irhamna, A.R.; Aziz, M. Production of ammonia as potential hydrogen carrier: Review on thermochemical and electrochemical processes. *Int. J. Hydrogen Energy* **2021**, *46*, 14455–14477. [CrossRef]
20. Berwal, P.; Kumar, S.; Khandelwal, B. A comprehensive review on synthesis, chemical kinetics, and practical application of ammonia as future fuel for combustion. *J. Energy Inst.* **2021**, *99*, 273–298. [CrossRef]
21. Gálvez, M.E.; Frei, A.; Halmann, M.; Steinfeld, A. Ammonia Production via a Two-Step Al_2O_3/AlN Thermochemical Cycle. *Ind. Eng. Chem. Res.* **2007**, *46*, 2047–2053. [CrossRef]
22. Li, K.; Chen, S.; Wang, H.; Wang, F. Plasma-assisted ammonia synthesis over Ni/LaOF: Dual active centers consisting of oxygen vacancies and Ni. *Appl. Catal. A Gen.* **2023**, *650*, 118983. [CrossRef]
23. Andersen, J.A.; Holm, M.C.; van't Veer, K.; Christensen, J.M.; Østberg, M.; Bogaerts, A.; Jensen, A.D. Plasma-catalytic ammonia synthesis in a dielectric barrier discharge reactor: A combined experimental study and kinetic modeling. *Chem. Eng. J.* **2023**, *457*, 141294. [CrossRef]

24. Sun, J.; Chen, Q.; Zhao, X.; Lin, H.; Qin, W. Kinetic investigation of plasma catalytic synthesis of ammonia: Insights into the role of excited states and plasma-enhanced surface chemistry. *Plasma Sources Sci. Technol.* **2022**, *31*, 094009. [CrossRef]
25. Engelmann, Y.; Kevin Yury Gorbanev Neyts, E.C.; Schneider, W.F.; Bogaerts, A. Plasma Catalysis for Ammonia Synthesis: A Microkinetic Modeling Study on the Contributions of Eley–Rideal Reactions. *ACS Publ.* **2021**, *9*, 13151–13163. [CrossRef]
26. Xie, P.; Yao, Y.; Huang, Z.; Liu, Z.; Zhang, J.; Li, T.; Wang, G.; Shahbazian-Yassar, R.; Hu, L.; Wang, C. Highly efficient decomposition of ammonia using high-entropy alloy catalysts. *Nat. Commun.* **2019**, *10*, 4011. [CrossRef] [PubMed]
27. Cui, G.; Zeng, W.; Li, Z.; Fu, Y.; Li, H.; Chen, J. Experimental study of minimum ignition energy of methane/air mixtures at elevated temperatures and pressures. *Fuel* **2016**, *175*, 257–263. [CrossRef]
28. Wang, D.; Ji, C.; Wang, S.; Yang, J.; Wang, Z. Numerical study of the premixed ammonia-hydrogen combustion under engine-relevant conditions. *Int. J. Hydrogen Energy* **2021**, *46*, 2667–2683. [CrossRef]
29. Xin, G.; Ji, C.; Wang, S.; Meng, H.; Chang, K.; Yang, J. Effect of different volume fractions of ammonia on the combustion and emission characteristics of the hydrogen-fueled engine. *Int. J. Hydrogen Energy* **2022**, *47*, 16297–16308. [CrossRef]
30. Lhuillier, C.; Brequigny, P.; Contino, F.; Mounaïm-Rousselle, C. Experimental investigation on ammonia combustion behavior in a spark-ignition engine by means of laminar and turbulent expanding flames. *Proc. Combust. Inst.* **2021**, *38*, 5859–5868. [CrossRef]
31. Han, X.; Wang, Z.; Costa, M.; Sun, Z.; He, Y.; Cen, K. Experimental and kinetic modeling study of laminar burning velocities of NH_3/air, NH_3/H_2/air, NH_3/CO/air and NH_3/CH_4/air premixed flames. *Combust. Flame* **2019**, *206*, 214–226. [CrossRef]
32. Jin, B.; Deng, Y.F.; Li, G.; Li, H. Experimental and numerical study of the laminar burning velocity of NH_3/H_2/air premixed flames at elevated pressure and temperature. *Int. J. Hydrogen Energy* **2022**, *47*, 36046–36057. [CrossRef]
33. Cai, T.; Zhao, D.; Gutmark, E. Overview of fundamental kinetic mechanisms and emission mitigation in ammonia combustion. *Chem. Eng. J.* **2023**, *458*, 141391. [CrossRef]
34. Chai, W.S.; Bao, Y.; Jin, P.; Tang, G.; Zhou, L. A review on ammonia, ammonia-hydrogen and ammonia-methane fuels. *Renew. Sustain. Energy Rev.* **2021**, *147*, 111254. [CrossRef]
35. Li, J.; Lai, S.; Chen, D.; Wu, R.; Kobayashi, N.; Deng, L.; Huang, H. A review on combustion characteristics of ammonia as a carbon-free fuel. *Front. Energy Res.* **2021**, *9*, 760356. [CrossRef]
36. Westlye, F.R.; Ivarsson, A.; Schramm, J. Experimental investigation of nitrogen based emissions from an ammonia fueled SI-engine. *Fuel* **2013**, *111*, 239–247. [CrossRef]
37. Mounaïm-Rousselle, C.; Bréquigny, P.; Dumand, C.; Houillé, S. Operating Limits for Ammonia Fuel Spark-Ignition Engine. *Energies* **2021**, *14*, 4141. [CrossRef]
38. Jin, S.; Wu, B.; Zi, Z.; Yang, P.; Shi, T.; Zhang, J. Effects of fuel injection strategy and ammonia energy ratio on combustion and emissions of ammonia-diesel dual-fuel engine. *Fuel* **2023**, *341*, 127668. [CrossRef]
39. Song, J.; Zello, V.; Boehman, A.L.; Waller, F.J. Comparison of the Impact of Intake Oxygen Enrichment and Fuel Oxygenation on Diesel Combustion and Emissions. *Energy Fuels* **2004**, *18*, 1282–1290. [CrossRef]
40. Maxwell, T.; Setty, V.; Jones, J.; Narayan, R. *The Effect of Oxygen Enriched Air on the Performance and Emissions of an Internal Combustion Engines*; SAE Technical Paper 932804; SAE International: Warrendale, PA, USA, 1993. [CrossRef]
41. Subramanian, K.; Ramesh, A. *Experimental Investigation on the Use of Water Diesel Emulsion with Oxygen Enriched Air in a DI Diesel Engine*; SAE Technical Paper 2001-01-0205; SAE International: Warrendale, PA, USA, 2001. [CrossRef]
42. Salzano, E.; Basco, A.; Cammarota, F.; Di Sarli, V.; Di Benedetto, A. Explosions of Syngas/CO_2 Mixtures in Oxygen-Enriched Air. *Ind. Eng. Chem. Res.* **2011**, *51*, 7671–7678. [CrossRef]
43. Baskar, P.; Senthilkumar, A. Effects of oxygen enriched combustion on pollution and performance characteristics of a diesel engine. *Eng. Sci. Technol. Int. J.* **2016**, *19*, 438–443. [CrossRef]
44. Li, S.-Q.; Guan, Q.; Zhang, W.-H. Test Study on Combustion Process of Oxygen-enriched Gasoline Engine. *J. Highw. Transp. Res. Dev.* **2008**, *3*, 25.
45. Liang, Y.; Shu, G.; Wei, H.; Zhang, W. Effect of oxygen enriched combustion and water–diesel emulsion on the performance and emissions of turbocharged diesel engine. *Energy Convers. Manag.* **2013**, *73*, 69–77. [CrossRef]
46. Karimi, M.; Wang, X.; Hamilton, J.; Negnevitsky, M. Numerical investigation on hydrogen-diesel dual-fuel engine improvements by oxygen enrichment. *Int. J. Hydrogen Energy* **2022**, *47*, 25418–25432. [CrossRef]
47. Mei, B.; Zhang, X.; Ma, S.; Cui, M.; Guo, H.; Cao, Z.; Li, Y. Experimental and kinetic modeling investigation on the laminar flame propagation of ammonia under oxygen enrichment and elevated pressure conditions. *Combust. Flame* **2019**, *210*, 236–246. [CrossRef]
48. Ganley, J.C.; Thomas, F.S.; Seebauer, E.G.; Masel, R.I. A Priori Catalytic Activity Correlations: The Difficult Case of Hydrogen Production from Ammonia. *Catal. Lett.* **2004**, *96*, 117–122. [CrossRef]
49. Comotti, M.; Frigo, S. Hydrogen generation system for ammonia–hydrogen fuelled internal combustion engines. *Int. J. Hydrogen Energy* **2015**, *40*, 10673–10686. [CrossRef]
50. Ryu, K.; Zacharakis-Jutz, G.E.; Kong, S.C. Performance enhancement of ammonia-fueled engine by using dissociation catalyst for hydrogen generation. *Int. J. Hydrogen Energy* **2014**, *39*, 2390–2398. [CrossRef]
51. Frigo, S.; Gentili, R.; Doveri, N. *Ammonia Plus Hydrogen as Fuel in a S.I. Engine: Experimental Results*; SAE Technical Paper 2012-32-0019; SAE International: Warrendale, PA, USA, 2012. [CrossRef]

52. Zhang, H.; Li, G.; Long, Y.; Zhang, Z.; Wei, W.; Zhou, M.; Belal, B.Y. Numerical study on combustion and emission characteristics of a spark-ignition ammonia engine added with hydrogen-rich gas from exhaust-fuel reforming. *Fuel* **2023**, *332*, 125939. [CrossRef]
53. Li, J.; Zhang, R.; Pan, J.; Wei, H.; Shu, G.; Chen, L. Ammonia and hydrogen blending effects on combustion stabilities in optical SI engines. *Energy Convers. Manag.* **2023**, *280*, 116827. [CrossRef]
54. Mei, B.; Zhang, J.; Shi, X.; Xi, Z.; Li, Y. Enhancement of ammonia combustion with partial fuel cracking strategy: Laminar flame propagation and kinetic modeling investigation of $NH_3/H_2/N_2$/air mixtures up to 10 atm. *Combust. Flame* **2021**, *231*, 111472. [CrossRef]
55. Lhuillier, C.; Brequigny, P.; Contino, F.; Mounaïm-Rousselle, C. Experimental study on ammonia/hydrogen/air combustion in spark ignition engine conditions. *Fuel* **2020**, *269*, 117448. [CrossRef]
56. Wang, Y.; Zhou, X.; Liu, L. Theoretical investigation of the combustion performance of ammonia/hydrogen mixtures on a marine diesel engine. *Int. J. Hydrogen Energy* **2021**, *46*, 14805–14812. [CrossRef]
57. Pochet, M.; Dias, V.; Moreau, B.; Foucher, F.; Jeanmart, H.; Contino, F. Experimental and numerical study, under LTC conditions, of ammonia ignition delay with and without hydrogen addition. *Proc. Combust. Inst.* **2019**, *37*, 621–629. [CrossRef]
58. Lin, Q.F.; Jiang, Y.M.; Liu, C.Z.; Chen, L.W.; Zhang, W.J.; Ding, J.; Li, J.G. Instantaneous hydrogen production from ammonia by non-thermal arc plasma combining with catalyst. *Energy Rep.* **2021**, *7*, 4064–4070. [CrossRef]
59. Gu, J.G.; Zhao, P.; Zhang, Y.; Wang, H.Y.; Jiang, W. Discharge Enhancement Phenomenon and Streamer Control in Dielectric Barrier Discharge with Many Pores. *Catalysts* **2020**, *10*, 68. [CrossRef]
60. Mei, D.H.; Fang, C.; Shao, T. Recent Progress on Characteristics and Applications of Atmospheric Pressure Low Temperature Plasmas. *Chin. J. Electr. Eng.* **2020**, *40*, 1339–1358+1425.
61. Ju, Y.; Sun, W. Plasma assisted combustion: Dynamics and chemistry. *Prog. Energy Combust. Sci.* **2015**, *48*, 21–83. [CrossRef]
62. Wolk, B.; DeFilippo, A.; Chen, J.Y.; Dibble, R.; Nishiyama, A.; Ikeda, Y. Enhancement of flame development by microwave-assisted spark ignition in constant volume combustion chamber. *Combust. Flame* **2013**, *160*, 1225–1234. [CrossRef]
63. Mariani, A.; Foucher, F. Radio frequency spark plug: An ignition system for modern internal combustion engines. *Appl. Energy* **2014**, *122*, 151–161. [CrossRef]
64. Morsy, M.H. Review and recent developments of laser ignition for internal combustion engines applications. *Renew. Sustain. Energy Rev.* **2012**, *16*, 4849–4875. [CrossRef]
65. Cathey, C.; Tang, T.; Shiraishi, T.; Urushihara, T.; Kuthi, A.; Gundersen, M.A. Nanosecond Plasma Ignition for Improved Performance of an Internal Combustion Engine. *IEEE Trans. Plasma Sci.* **2007**, *35*, 1664–1668. [CrossRef]
66. Wang, F.; Liu, J.B.; Sinibaldi, J.; Brophy, C.; Kuthi, A.; Jiang, C.; Ronney, P.; Gundersen, M. Transient plasma ignition of quiescent and flowing air/fuel mixtures. *IEEE Trans. Plasma Sci.* **2004**, *33*, 844–849. [CrossRef]
67. Barleon, N.; Cheng, L.; Cuenot, B.; Vermorel, O.; Bourdon, A. Investigation of the impact of NRP discharge frequency on the ignition of a lean methane-air mixture using fully coupled plasma-combustion numerical simulations. *Proc. Combust. Inst.* **2022**, *39*, 5521–5530. [CrossRef]
68. Mao, X.; Rousso, A.; Chen, Q.; Ju, Y. Numerical modeling of ignition enhancement of CH_4/O_2/He mixtures using a hybrid repetitive nanosecond and DC discharge. *Proc. Combust. Inst.* **2019**, *37*, 5545–5552. [CrossRef]
69. Wang, Y.; Guo, P.; Chen, H.; Chen, Z. Numerical modeling of ignition enhancement using repetitive nanosecond discharge in a hydrogen/air mixture I: Calculations assuming homogeneous ignition. *J. Phys. D Appl. Phys.* **2020**, *54*, 065501. [CrossRef]
70. Mao, X.; Chen, Q.; Guo, C. Methane pyrolysis with N_2/Ar/He diluents in a repetitively-pulsed nanosecond discharge: Kinetics development for plasma assisted combustion and fuel reforming. *Energy Convers. Manag.* **2019**, *200*, 112018. [CrossRef]
71. Snoeckx, R.; Cha, M.S. Inevitable chemical effect of balance gas in low temperature plasma assisted combustion. *Combust. Flame* **2021**, *225*, 1–4. [CrossRef]
72. Hwang, J.; Kim, W.; Agarwal, A.K.; Choe, W.; Cha, J.; Woo, S. Application of a novel microwave-assisted plasma ignition system in a direct injection gasoline engine. *Appl. Energy* **2017**, *205*, 562–576. [CrossRef]
73. José Martín Pastor Garcia-Oliver, J.M.; García, A.G.; Micó, C. Combustion improvement and pollutants reduction with diesel-gasoline blends by means of a highly tunable laser plasma induced ignition system. *J. Clean. Prod.* **2020**, *271*, 122499.
74. Merotto, L.; Balmelli, M.; Vera-Tudela, W.; Soltic, P. Comparison of ignition and early flame propagation in methane/air mixtures using nanosecond repetitively pulsed discharge and inductive ignition in a pre-chamber setup under engine relevant conditions. *Combust. Flame* **2022**, *237*, 111851. [CrossRef]
75. Zhang, S.; Oehrlein, G.S. From thermal catalysis to plasma catalysis: A review of surface processes and their characterizations. *J. Phys. D Appl. Phys.* **2021**, *54*, 213001. [CrossRef]
76. Wang, L.; Zhao, Y.; Liu, C.; Gong, W.; Guo, H. Plasma driven ammonia decomposition on a Fe-catalyst: Eliminating surface nitrogen poisoning. *Chem. Commun.* **2013**, *49*, 3787–3789. [CrossRef]
77. Wang, L.; Yi, Y.; Guo, Y.; Zhao, Y.; Zhang, J.; Guo, H. Synergy of DBD plasma and Fe-based catalyst in NH_3 decomposition: Plasma enhancing adsorption step. *Plasma Process. Polym.* **2017**, *14*, 1600111. [CrossRef]
78. Faingold, G.; Lefkowitz, J.K. A numerical investigation of NH_3/O_2/He ignition limits in a non-thermal plasma. *Proc. Combust. Inst.* **2021**, *38*, 6661–6669. [CrossRef]

79. Lin, Q.; Jiang, Y.; Liu, C.; Chen, L.; Zhang, W.; Ding, J.; Li, J. Controllable NO emission and high flame performance of ammonia combustion assisted by non-equilibrium plasma. *Fuel* **2022**, *319*, 123818. [CrossRef]
80. Choe, J.; Sun, W.; Ombrello, T.; Carter, C. Plasma assisted ammonia combustion: Simultaneous NOx reduction and flame enhancement. *Combust. Flame* **2021**, *228*, 430–432. [CrossRef]
81. Taneja, T.S.; Johnson, P.N.; Yang, S. Nanosecond pulsed plasma assisted combustion of ammonia-air mixtures: Effects on ignition delays and NOx emission. *Combust. Flame* **2022**, *245*, 112327. [CrossRef]
82. Shahsavari, M.; Konnov, A.A.; Valera-Medina, A.; Jangi, M. On nanosecond plasma-assisted ammonia combustion: Effects of pulse and mixture properties. *Combust. Flame* **2022**, *245*, 112368. [CrossRef]